

Supplemental Material for
Predicting point defect equilibria across oxide hetero-interfaces: model
system of $\text{ZrO}_2/\text{Cr}_2\text{O}_3$

Jing Yang^{a,b}, Mostafa Youssef^{a,b,c}, Bilge Yildiz^{a,b,c*}

^aLaboratory for Electrochemical Interfaces,

^bDepartment of Materials Science and Engineering

^cDepartment of Nuclear Science and Engineering, Massachusetts Institute of Technology, 77
Massachusetts Avenue, Cambridge, MA 02139, USA.

*Correspondence to: byildiz@mit.edu

List of contents:

1. Stability test of the constructed interface
2. Solution scheme of the continuum model
3. Derivation of defect concentration expression
4. Defect chemistry results at 800K

1. Stability test of the constructed interface

In order to test the stability of our constructed interface, we performed molecular dynamics (MD) calculation on the relaxed slab. MD calculation is performed at 600K for 1 ps, with a 2-fs time step. Comparing the final structure (Fig. S1) below with the initial structure (Fig. 2(c)) in the paper, we can see that the slab remains intact, with only small distortions at the interface, which implies that this interface is a stable configuration.

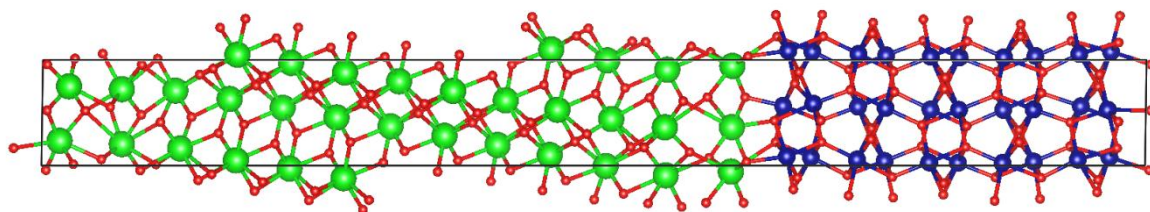


Figure S1. $m\text{-ZrO}_2$ (001)/ Cr_2O_3 (1-102) slab after 1ps MD. Oxygen ions are drawn small and red, Cr ions medium-sized and blue, Zr ions largest and green.

2. Solution scheme of the continuum model

This section gives a detailed description of the solution scheme we built for solving the continuum model. Fig. S2 (a) shows the geometry of the model we have built, where two core regions with non-zero segregation energy are defined (core 1 and core 2). As such, there are 3 boundaries in the interfacial region: boundary A between region 1 and core 1, boundary B between core 1 and core 2, and boundary C between core 2 and region 2. We define the potential drop in each of the four regions as $\Delta\phi_1$, $\Delta\phi_1^{core}$, $\Delta\phi_2^{core}$ and $\Delta\phi_2$ respectively, as in Fig. S2(b). The total potential drop $\phi_{built-in} = \Delta\phi_1 + \Delta\phi_1^{core} + \Delta\phi_2^{core} + \Delta\phi_2$.

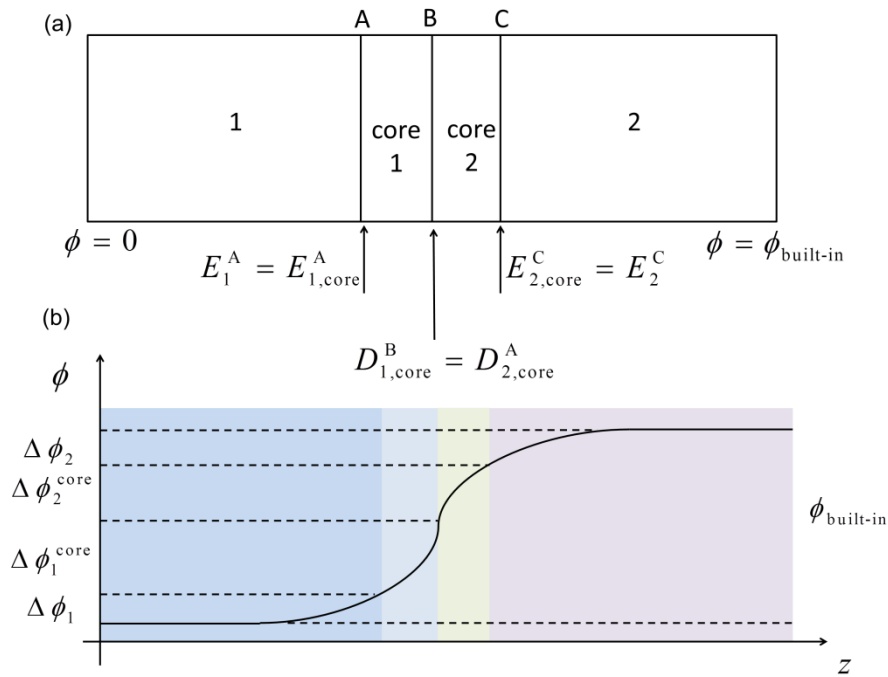


Figure S2. (a) Geometry and Boundary condition for the continuum model. (b) Potential drop defined for the four regions. Four regions exist from left to right: region 1, region core 1, region core 2 and region 2. They represent the space charge layer of ZrO_2 , core region of ZrO_2 , core region of Cr_2O_3 , and space charge layer of Cr_2O_3 respectively. Boundary A forms between region 1 and core 1, boundary B core 1 and core 2, and boundary C core 2 and

region 2. At each of the boundary, we annotate the electric field E as $E_{\text{region}}^{\text{boundary}}$. For example, $E_{1,\text{core}}^{\text{A}}$ represents the left-sided limit of E at boundary A. Same notation is used for the electric displacement field D . Potential drop in each of the four regions are annotated as $\Delta\phi_1$, $\Delta\phi_1^{\text{core}}$, $\Delta\phi_2^{\text{core}}$, $\Delta\phi_2$.

Far away from the interface local charge neutrality should be achieved. From the bulk defect equilibria calculation we have obtained the electron chemical potential (Fermi level) that achieves charge neutrality, μ_e^1 and μ_e^2 . We need to align the bands on the two sides to get the relative position of μ_e^1 and μ_e^2 . Here we assume that the valence band offset we calculated from Eq. 9 in the paper is the difference in valence band edges at boundary A and C, i.e.

$$E_v^{\text{boundaryA}} - E_v^{\text{boundaryC}} = \Delta E_v^{\text{ZrO}_2 - \text{Cr}_2\text{O}_3}. \quad (1)$$

The valence band positions in the bulk regions are

$$E_v^{z=0} = E_v^{\text{boundaryA}} + \Delta\phi_1, \quad (2)$$

$$E_v^{z=L} = E_v^{\text{boundaryC}} - \Delta\phi_2. \quad (3)$$

The equilibrium condition of flat electron chemical potential requires

$$E_v^{z=0} + \mu_e^1 = E_v^{z=L} + \mu_e^2. \quad (4)$$

Combining Eq. 1-4, we can arrive at the constraint that

$$\Delta\phi_1 + \Delta\phi_2 = \mu_e^2 - \mu_e^1 - \Delta E_v^{\text{ZrO}_2 - \text{Cr}_2\text{O}_3}. \quad (5)$$

We emphasize that the offset in the valence band calculated by DFT on the defect-free interface is assumed here to represent the difference in the valence band between boundary A and C as in Eq. 5 instead of representing the discontinuity of the valence band at boundary B.

The argument here is that calculating this offset is based on taking the difference in the

electrostatic potential in the two bulk-like regions where flat potential is achieved. These two bulk-like regions are located to the left of boundary A and to the right of boundary C. In between A and C (inclusive boundary B) the electrostatic potential is never flat as can be seen in Fig. 3(a) in the paper. As such any changes in the band offset inside the two core zones beyond what is evaluated between A and C is assumed here to be due to the presence of charged defects in these two regions.

With Eq. 5 and the continuity of electric field displacement, we have all the boundary conditions we need. We designed the solution scheme as follows:

- (1) Give an initial guess of $\Delta\phi_1$. (With Eq. 5, this also determines the value of $\Delta\phi_2$.)
- (2) Solve Poisson's equation for region 1 and region 2, and calculate electric fields E_1^A and E_2^C .
- (3) Iterate over $\Delta\phi_1^{core}$, solve Poisson's equation for core 1 until $E_1^A = E_{1,core}^A$ is reached at boundary A.
- (4) Iterate over $\Delta\phi_2^{core}$, solve Poisson's equation for core 2 until $E_{2,core}^C = E_2^C$ is reached at boundary C.
- (5) With all the four regions solved, integrate the charge concentration $\rho_{tot} = \int \rho(z) dz$. If ρ_{tot} equals zero (within a chosen accuracy range), the problem is solved. If ρ_{tot} is not zero, give a new guess for $\Delta\phi_1$ and return to step (1).

It's noteworthy that the global charge neutrality condition is equivalent to the continuity of electric displacement field D at the interface, given that local charge neutrality is maintained and electric field is zero far away from the interface. This can be easily deduced from Poisson's equation $\rho(z) = \epsilon\epsilon_0 \frac{dE}{dz}$. On the left side integrating from $z=0$ to the interface, we

have the total charge on the left side

$$Q_1 = \varepsilon_0 \varepsilon_1 (\rho|_{z=0} + \int_0^{\text{interface}} \frac{dE}{dz} dz) = D_{1,\text{core}}^{\text{B}} . \quad (6)$$

Similarly, if we integrate from $z=L$ to the interface, we have the total charge on the right side

$$Q_2 = \varepsilon_0 \varepsilon_2 (\rho|_{z=L} - \int_{\text{interface}}^{z=L} \frac{dE}{dz} dz) = -D_{2,\text{core}}^{\text{B}} . \quad (7)$$

The global charge neutrality condition requires that $Q_1 + Q_2 = 0$, which is equivalent to $D_{1,\text{core}}^{\text{B}} = D_{2,\text{core}}^{\text{B}}$.

The dielectric constant for monoclinic ZrO_2 is taken as 20 as in our previous work.¹ We calculated the dielectric tensor of Cr_2O_3 using density-functional perturbation theory.² The calculation gives diagonal terms of 11.0 in a axis and 12.7 in c axis, and off-diagonal terms are 0. This result is in reasonable agreement with experimentally measured values (13.0 and 11.8).³ A constant value 12 is used for the Cr_2O_3 side for solving Poisson's equation.

3. Derivation of defect concentration expression

The equilibrium defect concentrations are determined by the minimization of Gibbs free energy. It has been shown that, when it comes to the interface system, this equilibrium condition is equivalent to a flattened electrochemical potential for the mobile species.⁴

The electrochemical potential of a charged defect D^q can be defined as⁵

$$\tilde{\mu}_{D^q} = \mu_0 + \mu_{\text{cig}} + q\phi . \quad (8)$$

Here μ_0 is the concentration-independent contribution. In the context of our DFT calculation where we ignore the formation entropies, $\mu_0 = E_{D^q}^{f,\text{bulk}} + \Delta E_{D^q}^f$. $\Delta E_{D^q}^f$ represents the energetic preference of defects segregating to or depleting from the interfacial core region

due to the bonding environment variation. ϕ is the electrostatic potential in the space-charge layer.

μ_{cfg} denotes the concentration-dependent contribution and it arises from the configurational entropy generated by the defect. A general form for this term is given by:

$$\mu_{\text{cfg}} = k_B T \ln\left(\gamma \frac{[\text{D}^q]}{1 - \sum_{q'} [\text{D}^{q'}]}\right). \quad (9)$$

The term $k_B T \ln\left(\frac{[\text{D}^q]}{1 - \sum_{q'} [\text{D}^{q'}]}\right)$ represents the dilute limit configurational entropy generated by the charge state q of the defect D. γ is the “empirical” activity coefficient that implicitly accounts for defect-defect interaction.

If we assume that in dilute limit, defect do not interact except for the mean-field electrostatic force, and that $[\text{D}^q] \ll 1$, we can get a simplified form

$$\mu_{\text{cfg}} = k_B T \ln([\text{D}^q]). \quad (10)$$

The drift-diffusion flux is defined by

$$J_{\text{D}^q} = -M_{\text{D}^q} \nabla \tilde{\mu}_{\text{D}^q}, \quad (11)$$

where M_{D^q} is the mobility. Assuming that there is no generation or annihilation of defect during the transport process, the transport equation is

$$\frac{\partial [\text{D}^q]}{\partial t} = -\nabla \cdot J_{\text{D}^q} \quad (12)$$

Under equilibrium, the fluxes of all species should be zero, which means the electrochemical potential is constant. Eq. 7 reduces to

$$J_{\text{D}^q} = 0 \quad (13)$$

The defect electrochemical potential in bulk using Eq. 10 is given by

$$\tilde{\mu}_{\text{D}^q}^{\text{bulk}} = E_{\text{D}^q}^{\text{f},\text{bulk}} + k_B T \ln([\text{D}^q]_{\text{bulk}}). \quad (14)$$

Since equilibrium is reached across the interface, $\tilde{\mu}_{D^q}(z)$ is equal to $\tilde{\mu}_{D^q}^{bulk}$ throughout the oxide material, we arrive at the equation for defect concentration

$$[D^q](z) = [D^q]_{bulk} \exp\left(-\frac{q\Delta\phi(z) + \Delta E_{D^q}^f}{k_B T}\right). \quad (15)$$

If Eq. 9 is used instead of Eq. 10 to represent the electrochemical potential of the defect D^q , such an analytical expression for defect concentration is not possible and the drift-diffusion equation needs to be solved numerically.

4. Defect chemistry results at 800K

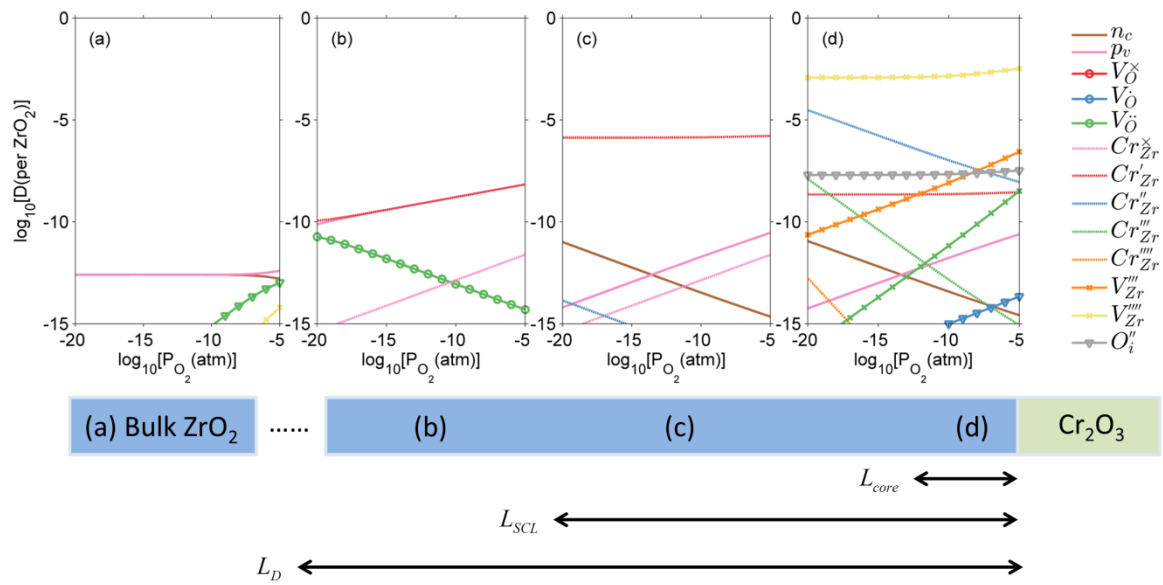


Figure S3. Defect concentrations in ZrO₂ (a) in bulk, (b) far from the space-charge zone but within the reach of Cr defects, (c) outside the core layer within the space-charge zone, and (d) in the core layer at 800K and different oxygen partial pressures.

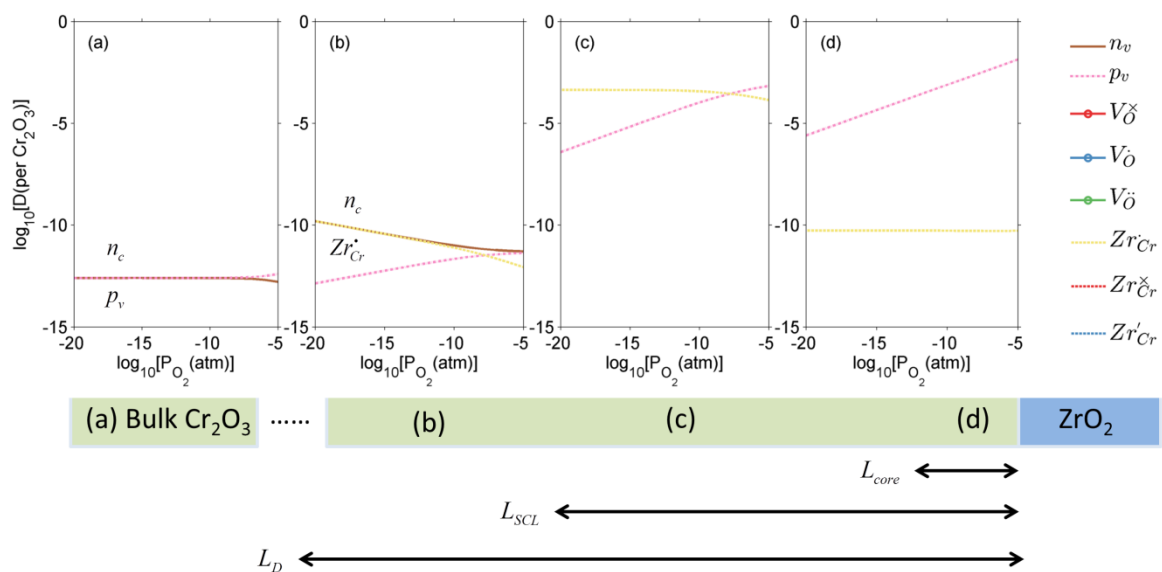


Figure S4. Defect concentrations in Cr_2O_3 (a) in bulk, (b) far from the space-charge zone but within the reach of Cr defects, (c) outside the core layer within the space-charge zone, and (d) in the core layer at 800K and different oxygen partial pressures.

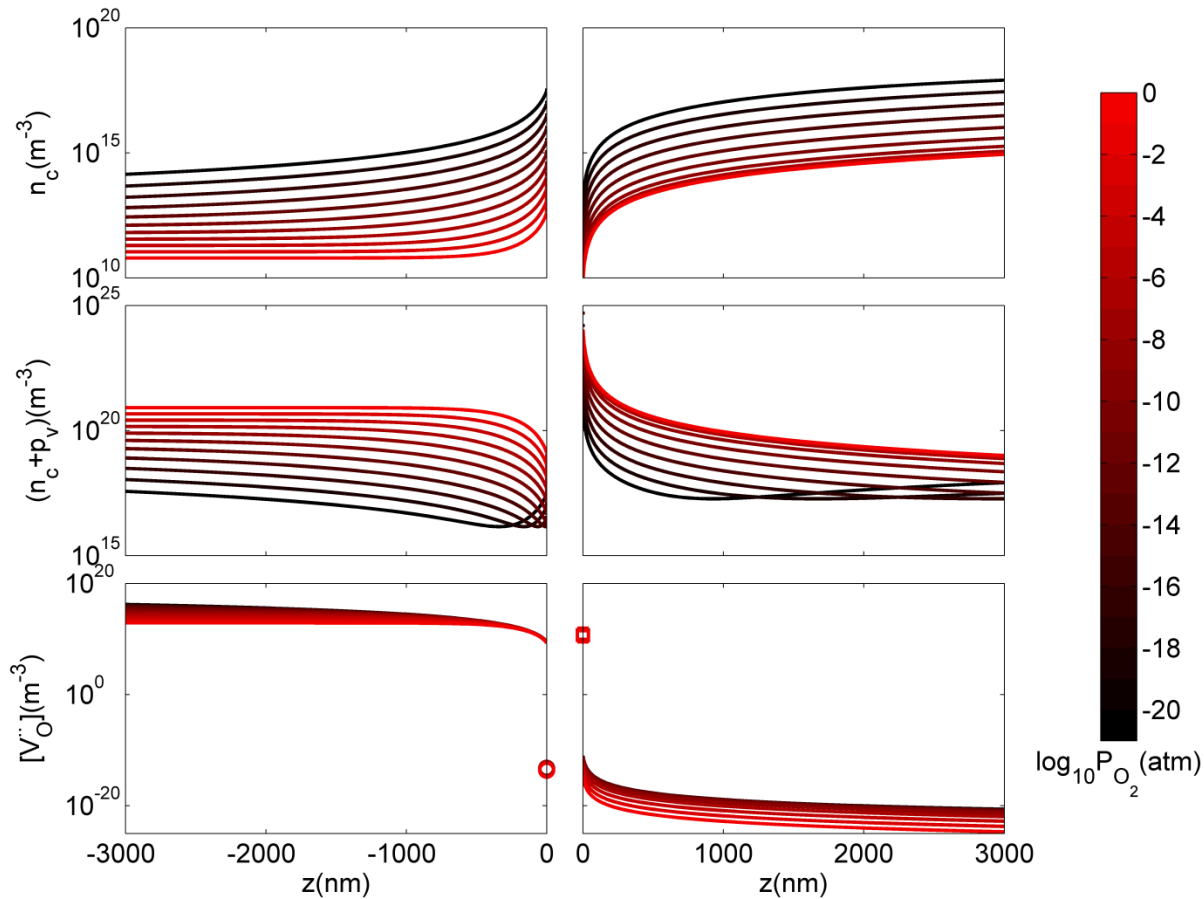


Figure S5. Spatially-resolved concentrations of (a) electrons, (b) sum of electrons and holes and (c) $V_o^{\bullet\bullet}$ as a function of oxygen partial pressure at T=800K. Circles and squares in panel (c) represent the concentrations in the core layer on the ZrO₂ and Cr₂O₃ sides, respectively.

1. M. Youssef, M. Yang and B. Yildiz, *Physical Review Applied* **5** (1), 014008 (2016).
2. S. Baroni, S. de Gironcoli, A. Dal Corso and P. Giannozzi, *Reviews of Modern Physics* **73** (2), 515-562 (2001).
3. P. H. Fang and W. S. Brower, *Physical Review* **129** (4), 1561-1561 (1963).
4. R. A. De Souza, *Physical Chemistry Chemical Physics* **11** (43), 9939-9969 (2009).
5. J. Maier, *Solid State Ionics* **143** (1), 17-23 (2001).